The Journal of Immunology

Self versus Nonself Discrimination by the Soluble Complement Regulators Factor H and FHL-1

Arthur Dopler, Leonie Guntau, Markus J. Harder, Annette Palmer, Britta Höchsmann, Hubert Schrezenmeier, Thomas Simmet, Markus Huber-Lang and Christoph Q. Schmidt

J Immunol 2019; 202:2082-2094; Prepublished online 11 February 2019;
doi: 10.4049/jimmunol.1801545
http://www.jimmunol.org/content/202/7/2082

The Journal of Immunology is published twice each month by
The American Association of Immunologists, Inc.,
1451 Rockville Pike, Suite 650, Rockville, MD 20852

Print ISSN: 0022-1767 Online ISSN: 1550-6606.

Self versus Nonself Discrimination by the Soluble Complement Regulators Factor H and FHL-1

Arthur Dopler,* Leonie Guntau,* Markus J. Harder,* Annette Palmer,† Britta Höchsmann,‡,§ Hubert Schrezenmeier,‡,§ Thomas Simmet,* Markus Huber-Lang,† and Christoph Q. Schmidt*

The plasma proteins Factor H (FH) and its alternate splice variant FH-like protein 1 (FHL-1) are the major regulators of the complement alternative pathway. The indiscriminate nature of alternative pathway activation necessitates the regulators to be host selective, but the underlying principles of selectivity remained largely elusive. By analyzing human FH and FHL-1 for protection of different host and foreign cells (rabbit and yeast), we uncovered a 2-fold discriminatory mechanism of FH in favor of self: relative to FHL-1, FH exhibits a regulatory benefit on self but importantly, also, a regulatory penalty on nonself surfaces, yielding a selectivity factor of ∼2.4 for sialylated host surfaces. We further show that FHL-1 possesses higher regulatory activity than known but is relatively unselective. The reason for this unexpected high activity of FHL-1 is the observation that the complement regulatory site in FH exceeds the established first four domains. Affinity for C3b, cofactor and decay-accelerating activities, and serum assays demonstrate that the regulatory site extends domains 1–4 and includes domains 5–7. But unlike FH, FHL-1 exhibits a fast plasma clearance in mice, occurs sparsely in human plasma (at one fortieth of the FH concentration), and resists deregulation by FH-related proteins. These physiological differences and its late phylogenetic occurrence argue that FHL-1 is crucial for local rather than systemic compartments. In conclusion, we demonstrate a 2-fold discriminatory power of FH to promote selectivity for self over foreign and show that FHL-1 is more active than known but specialized for regulation on local tissues. ***The Journal of Immunology*****, 2019, 202: 2082–2094.**

The complement system is an integral part of the innate immune system. Its immune surveillance functions participate in protecting the host from pathogen invasion but are also important for other physiological roles like the maintenance of tissue homeostasis (1). As for any immune effector, the distinction between self and nonself is of fundamental importance. The two complement activation routes of the classical pathway (CP) and the lectin pathway (LP) are specific because they are triggered upon recognition of selective danger patterns, such as Ab–antigen complexes or foreign carbohydrates, respectively. Although recognition of particular stimuli has the advantage of being specific for the target, the immune system as a whole would require an infinitely large repertoire of versatile sensors to cover all possible dangerous structures.

To complement the more specific recognition by CP/LP and to achieve a very broad target range, our phylogenetically old defense mechanism, the complement alternative pathway (AP), enables the perpetual targeting of any possible (bio)surface available. C3 autoactivates at a low level through a conformational change, called tick-over, and thus provides permanent immune surveillance via the AP (2, 3). The indiscriminate nature of the AP is achieved by the central complement protein C3, which can covalently attach to any nucleophile (e.g., on proteins or carbohydrates) as soon as it is activated. C3 autoactivation and indiscriminate surface attachment paired with C3b self-amplification via the AP amplification loop facilitates a constant and incredibly broad surveillance of targets but also holds the risk of damaging our self surfaces (4). To avoid such self-harming, host surfaces are equipped with preformed complement regulators (reviewed in Refs. 5, 6). Because the activation of the AP is not per se selective for "foreign," the regulation of the AP needs to be specific for self-surfaces, otherwise microbial intruders could obtain erroneous protection. Host cells are equipped with several membrane-tethered complement regulators and thus occur specifically only on self-cells. However, cell membrane–fixed regulators are not sufficient for host-specific AP control. Host cells, but most specifically the specialized basement membranes of the fenestrated endothelium in the eye and the kidney, which are built from proteoglycans and cannot express cell membrane–fixed regulators, require additional protection by the soluble regulator Factor H (FH) and/or its splice version, FH-like

*Institute of Pharmacology of Natural Products and Clinical Pharmacology, Ulm University, 89081 Ulm, Germany; †Institute of Clinical and Experimental Trauma-Immunology, University Hospital, 89081 Ulm, Germany; ‡Institute of Transfusion Medicine, University of Ulm, 89081 Ulm, Germany; and §Institute for Clinical Transfusion Medicine and Immunogenetics, German Red Cross Blood Transfusion Service Baden-Wurttemberg-Hessen and University Hospital, 89081 Ulm, Germany

ORCID: 0000-0003-3137-0939 (L.G.).

Received for publication November 21, 2018. Accepted for publication January 14, 2019.

This work was supported by Deutsche Forschungsgemeinschaft Grant SCHM3018/2-2 (to C.Q.S.).

C.Q.S. and M.H.-L. conceived the study. A.D., L.G., M.J.H., C.Q.S., and A.P. performed the experiments. H.S., T.S., and B.H. advised on experimental design and data analysis. A.D., L.G., C.Q.S., and M.J.H. prepared the protein reagents. All authors contributed to the discussion of the data. The manuscript was written by A.D. and C.Q.S.; all authors critically revised the manuscript.

Address correspondence and reprint requests to Dr. Christoph Q. Schmidt, Institute of Pharmacology of Natural Products and Clinical Pharmacology, Ulm University, Helmholtzstraße 20, 89081 Ulm, Germany. E-mail address: christoph.schmidt@uni-ulm.de

The online version of this article contains supplemental material.

Abbreviations used in this article: AP, alternative pathway; CA, cofactor activity; CCP, complement control protein; CP, classical pathway; DAA, decay-accelerating activity; FB, Factor B; FD, Factor D; FH, Factor H; FHL-1, FH-like protein 1; FHR, FH-related protein; GAG, glycosaminoglycan; LP, lectin pathway; NHS, normal human serum; PBST, PBS containing 0.05% Tween 20; PNH, paroxysmal nocturnal hemoglobinuria; RU, response unit; SPR, surface plasmon resonance.

protein 1 (FHL-1). Apart from controlling the consumption of the AP in the fluid phase, FH associates with polyanionic host markers like sialic acids and glycosaminoglycans (GAGs) on our host surfaces to reinforce/provide protection from complement attack.

FH is built solely from 20 complement control protein (CCP) domains and contains two binding regions for C3b at either terminus and two binding regions for polyanionic host markers (Fig. 1A) (7). The first C3b binding site locates to CCP domains 1–4 and contains the complement regulatory functions of cofactor activity ([CA] for the Factor I–mediated degradation of C3b) and decay-accelerating activity ([DAA] for limiting the life span of the C3bBb convertase) (reviewed in Refs. 5, 8). Whereas CCP 7 contains a GAG recognition site (with contributions of neighboring domains) but does not bind sialic acids (9–13), CCPs 19–20 contain another C3b binding site as well as GAG and sialic acid recognition sites (7, 11, 14–18). The alternative splicing product of the FH gene, FHL-1 contains only the first seven CCP domains, followed by four unique amino acids (see Fig. 1A) (19–21). Thus, FHL-1 harbors the N-terminal FH regulatory site and one GAG recognition site, but lacks the C-terminal C3b-binding and self-recognition domains 19–20, which are known to be most critical for self-protection by FH (22–27). It is known that FH has a regulatory benefit on surfaces with host or hostlike polyanions to differentiate between self and foreign, but the mechanism of how this specificity is achieved, and how high the specificity factor on sialylated human surfaces is, has remained elusive. Similarly, the physiological role of the splice variant FHL-1 in AP control, as well as its implicated pathophysiological roles in age-related macular degeneration (AMD) and cancer, remain unresolved.

By determining the regulatory activities of FH and FHL-1 for protection of several different host and foreign surfaces, we uncovered that FH features a 2-fold discriminatory power in favor of self: relative to FHL-1, FH exhibits a regulatory benefit on self but importantly, also, a regulatory penalty on nonself surfaces. This two-sided discriminatory mechanism increases the selectivity and hence the safety margin for host over foreign. Moreover, our study 1) establishes the reasons why the splice variant FHL-1 exhibits unexpected high regulatory activity toward the AP despite the lack of 13 C-terminal FH domains, 2) shows that FHL-1 exhibits regulatory features that are distinct from FH, 3) determines that the FHL-1 concentration in circulation is very low, and 4) elaborates that FHL-1 is tailored for AP regulation on specialized, local tissues rather than the systemic circulation.

Materials and Methods

Human blood components

Fresh paroxysmal nocturnal hemoglobinuria (PNH)–RBCs from patients under eculizumab treatment were used under approval by the Ethical Committee of Ulm University. Sera were collected in VACUETTE/S-Monovette serum collection tubes, aliquoted, frozen in liquid nitrogen, and stored at −80°C. Standardized normal human serum (NHS) and FH-depleted serum, which is also depleted of FHL-1 (see Fig. 8), were obtained from CompTech.

Proteins

If not stated otherwise, all complement proteins like FH, C3b, Factor B (FB), and Factor D (FD) were purchased from CompTech as plasma purified proteins. The N-terminal FH fragments FH1-4, FH1-5, FH1-6; the splice variant FHL-1; and the FH-related (FHR)–1 protein were produced recombinantly in *Pichia pastoris* as described before (28), with small modifications. All proteins were stored in PBS except for the concentrated FHL-1 stock at 45–122 μM, which was dissolved in glycine buffer containing 20 mM glycine and 150 mM NaCl (pH 10.5). FHL-1 was prediluted from the stock into PBS prior to each assay to reach the appropriate concentration needed for the specific assay. The final dilution of FHL-1 stock into the assay condition was at least 1:3, and in control reactions, we ruled out that the same dilution of glycine buffer into PBS had an effect on the assay other than PBS alone.

Yeast opsonization assay

A Zeocin-resistant *P. pastoris* KM71H clone was grown overnight in 10 ml yeast extract, peptone, dextrose medium, spun down, and diluted with PBS to an OD_{600} of 1. To block CP/LP activation, serum was supplemented with 12.5 mM Mg-EGTA. Subsequently, 20 μl PBS or PBS spiked with analytes was mixed with 20 μl serum (40% final serum content) and 10 μl yeast suspension and incubated for 1 h at 37°C. After incubation, cells were washed with 400 μl PBS twice and incubated for 10 min with 50 μl of a dilution of biotinylated anti-C3d Ab (Quidel) (1:100) in PBS. Unbound Ab was removed in another wash step with 400 μl PBS; then, cells were labeled with 50 μl allophycocyanin-conjugated streptavidin (1:100 in PBS) for 30 min. Following a last wash step (400 μl PBS), opsonized cells were analyzed with flow cytometry (BD FACSVerse).

Cell culture

Human microvascular endothelial cells (HMEC-1; ATCC) were grown in MCDB 131 medium (Life Technologies) supplemented with 10% FCS (Life Technologies), 2 mM glutamine (Biochrom), 100 U/ml penicillin and 100 μg/ml streptomycin (Life Technologies), 1 μg/ml hydrocortisone (Rotexmedica), and 10 ng/ml recombinant human epidermal growth factor (Sigma-Aldrich) at 37°C and 5% CO_2.

Endothelial cell opsonization assay

HMEC-1 cells, cultured for 2 d in a culture flask, were exposed to serum diluted into PBS and supplemented with 1 mM $MgCl_2$ spiked with analytes (40% final serum content) in a final volume of 300 μl for 1 h at 37°C. After incubation, the cells were detached with trypsin/EDTA and opsonized cells were labeled with biotinylated anti-C3d and allophycocyanin-conjugated streptavidin, as already described for the yeast opsonization assay. C3d is resistant to trypsin digestion (29). IC_{50} values were calculated for every single experiment by fitting the data to a nonlinear regression using the software GraphPad Prism. The IC_{50} of every individual experiment was fitted individually and the mean and SD of the IC_{50} values were calculated for every group.

PNH erythrocyte hemolysis assay

Erythrocytes from whole blood of PNH patients (collected in EDTA) were washed with PBS thrice. For experiments with desialylated erythrocytes, 100 μl of cell suspension was treated with 36 U neuraminidase (New England Biolabs) for 1 h at 37°C. After incubation, 10 μl of (de)sialylated erythrocytes and 10 μl of 25 mM Mg-EGTA were mixed with 20 μl FH/FHL-1–depleted serum that was supplemented with analytes (alternatively, as controls NHS or heat-inactivated serum were used). The reaction mixture was incubated at 37°C overnight and stopped by addition of 150 μl ice-cold 5 mM EDTA in PBS. Finally, cells were spun down, and absorbance of the supernatants was measured at 405 nm. Hemolysis was calculated as the quotient of measured absorption of the sample and total lysis in water (100% reference). IC_{50} values were calculated for every single experiment by fitting the data to a nonlinear regression using the software GraphPad Prism. The IC_{50} values of every individual experiment were fitted individually and the mean and SD of the IC_{50} values were calculated for every group.

Rabbit erythrocyte hemolysis assay

Rabbit erythrocytes (Fiebig Nährstofftechnik) were supplied in Alsever solution and washed with PBS. Then, 10 μl of a suspension was mixed with 20 μl serum, 10 μl of 25 mM Mg-EGTA in PBS, and 10 μl of PBS or analytes diluted in PBS. The reactions were incubated for 30 min at 37°C and stopped with 150 μl ice-cold PBS supplemented with 5 mM EDTA. Finally, cells were spun down, and absorbance of the supernatants was measured at 405 nm. Hemolysis was calculated as the quotient of measured absorption of the sample and total lysis in water (100% reference).

FH/FHL-1 detection in serum

Because FH and FHL-1 are very similar, it is impossible to measure the serum concentrations separately using ELISA due to the lack of specific mAbs to date. Instead, we performed a Western blot analysis with 5% serum samples and used standards to estimate the concentrations in the serum. As standards, a series of purified FH and FHL-1 (CompTech) preparations at defined concentrations were added into a dilution of FH-depleted serum in PBS (final serum content 5%). The serum samples or the reference samples with defined FH and FHL-1 concentrations in FH-depleted serum (final serum content always 5%) were run on on a 4–12% Bis-Tris gradient SDS-PAGE gel (Invitrogen) under nonreducing conditions. Proteins were transferred to a PVDF membrane followed by blocking with 5% (w/v)

nonfat dry milk in PBS for 1 h. A murine anti-human FH (clone 90×; Quidel) Ab binding to CCP1 of FH and FHL-1 was diluted 1:1000 in blocking buffer and incubated with the membrane overnight. Afterwards, an ovine HRP-coupled anti-mouse $F(ab')_2$ fragment (GE Healthcare) was used as a secondary reagent in a dilution of 1:2500 in blocking buffer and incubated for 1 h with the membrane. Proteins were visualized in an imaging system (Amersham Imager 680) after exposure to ECL prime Western blotting detection reagent (GE Healthcare). Signal intensities were compared with the standard series to estimate the protein concentration in serum.

Determination of terminal plasma half-life

The terminal plasma half-life of FH and FHL-1 was assessed in male C57BL/6 mice. Mice at an age of 6–8 wk were anesthetized with sevofluran (Abbott Laboratories) and a single dose of 60 or 100 μg of sterile, endotoxin-free protein in PBS (FH or FHL-1; four mice per group) was injected into the penile vein. At the given time points, blood samples were taken by puncture of the tail vein, and the blood was immediately diluted 1 in 2 with PBS containing 10 mM EDTA. The blood was centrifuged, and the plasma was stored at −80°C until quantification. After 72 h, the mice were killed by inhalation anesthesia with sevofluran and terminal bleeding by puncture of the left ventricle. All animal experiments were performed in compliance with the guidelines of the German Animal Protection Act and were approved by the Regierungspräsidium Tübingen (Tübingen, Germany).

Serum samples were analyzed in a sandwich ELISA. High binding microtiter plates (MaxiSorp; Nunc) were coated with 50 μl of a dilution of mouse anti-human FH Ab (0.5 μg/well; Thermo Fisher Scientific clone C18/3 for FH or Quidel clone 90× for FHL-1) for 2 h, followed by washing with 200 μl PBS containing 0.05% Tween 20 ([PBST] Appli-Chem) twice. Unspecific binding sites were blocked with 200 μl PBS/BSA (PBS containing 1% BSA) for 1 h. The murine plasma samples or a dilution series (1:2) of the reference samples of FH or FHL-1 (previously diluted in serum of untreated mice) were prepared with PBS/BSA (duplicates) and added (50 μl) to the Ab-coated plates and incubated for 30 min (the highest reference point of the dilution series has a concentration of 500 ng/ml FH or FHL-1). Plates were washed three times with 200 μl PBST. Then, 50 μl of a 1:1000 diluted (PBS/BSA) goat anti-human FH polyclonal Ab (CompTech) was added to the wells. After 30 min incubation and a wash step (3 × 200 μl PBST), the wells were exposed to 50 μl of a donkey anti-goat IgG HRP (1:2000 in PBS/BSA; Abcam) for 30 min. Finally, the wells were washed three times with 200 μl PBST and absorbance was measured at 405 nm after addition of 50 μl freshly prepared detection reagent containing ABTS (0.5 mg/ml, Roche) and 0.03% H_2O_2 in 100 mM sodium citrate (pH 4.3). Plotting the standard series concentration after blank value subtraction (i.e., wells incubated without sample and secondary Ab) resulted in an exponential regression line, and the corresponding equation was used to calculate the serum concentration of the sample dilution series. Only values in the linear range were taken into account. Linear regression curves were calculated for the concentration–time plots based upon data points that were linear (β-phase). Terminal plasma half-life values were determined from these equations for every individual mouse and the mean and SD were calculated for every group.

Binding affinity to C3b

The affinity of FHL-1 and the derived fragments to C3b was measured with surface plasmon resonance (SPR) spectroscopy according to previously published methods (30–32) with a Reichert SPR7500DC SPR spectrometer (all experiments at 25°C). Briefly, a carboxymethyldextran hydrogel biosensor chip (CMD500 m; XanTec) was conditioned and washed according to manufacturer recommendations before C3b was covalently attached to the surface by standard amine coupling to one of the flow cells. In total, 3500–5500 response units (RUs) of C3b were immobilized on the chip. All binding experiments were performed at a flow rate of 25 μl/min and protein series (1 in 2 dilution) were prepared in running buffer (FH1-4, FH1-5 from 40 μM to 313 nM; FH1-6 from 40 μM to 156 nM; and FHL-1 from 5 μM to 20 nM). After injection of analytes for 3 min, buffer was flown over the chip and dissociation was observed for 5 min. For regeneration, 1 M NaCl was injected for 0.5 min followed by 4 min buffer flow. Only reference subtracted sensorgrams are shown. Plots of response at steady state versus concentration were used for calculation of equilibrium dissociation constants K_D (TraceDrawer software, 1:1 steady-state affinity model).

Decay acceleration assay

For the quantification of the DAA of FH, the N-terminal FH truncations and FHL-1 SPR were used, following an established method (30, 33). Briefly, C3b was immobilized on a CMD500 m biosensor chip (XanTec) by amine coupling. The amine-coupled molecules were used as a starting point for the formation of convertases. For this purpose, FB and FD were diluted with running buffer (PBS with 0.005% [v/v] Tween 20 and 1 mM $MgCl_2$) to 600 and 100 nM, respectively, and injected together for 3 min. Convertases that were build up on the chip were allowed to naturally decay for 1 min, which was then accelerated by injection of the analytes for 3.5 min. Residual convertases and analytes were removed by injection of CR1 CCP1-3 for 2.5 min and 1 M NaCl for another 0.5 min. To show the DAA of the analytes alone, responses resulting through binding of analyte to C3b in absence of convertase were subtracted from the response of convertase decay. Only reference-subtracted sensorgrams are shown.

Fluid phase CA assay

This assay was conducted as previously described (28, 30, 34). In brief, C3b (0.7 μM), Factor I (0.01 μM), and the analytes (0.1 μM) were mixed with PBS (20 μl total volume) and incubated on a rotary shaker (60 rpm) at 37°C for 10, 20, 40, and 80 min. Addition of 5 μl reducing SDS-PAGE sample buffer stopped the reactions, and samples were analyzed on 9% SDS-PAGE gels subsequently. Gels were stained with Coomassie Brilliant Blue R250 (Sigma-Aldrich) and densitometric analysis of the bands was performed with the software ImageJ after imaging (Amersham Imager 680). A negative control without cofactor was used to normalize the intensities of the samples incubated with analyte.

In silico gene analysis

The human FH gene was accessed at Ensembl [release 90 (35)], and FH genes of other species were obtained from the National Center for Biotechnology Information gene database or nucleotide database. A representative number of primates with species from different orders and the two common laboratory animals, mouse and rat, were chosen for analysis. The exon structure of every FH gene that had not been assigned yet was analyzed in silico. Each exon of the human FH gene was aligned with the whole FH gene of the individual species to identify the positions of the exons using the European Molecular Biology Open Software Suite Needleman-Wunsch algorithm of the European Bioinformatics Institute web service. The identified exons were then compared with the correlating human exons for their identity score using the European Molecular Biology Open Software Suite Needle-Wunsch algorithm. Exons were also translated to their corresponding amino acid sequences with the ExPASy translate tool and compared with each other using the abovementioned algorithm. In order to define whether the splice variant FHL-1 occurs in a species, we screened the species for an exon similar to human FH exon 10, which codes for the unique peptide tail SFTL of FHL-1 followed by a stop codon. For this purpose, we aligned the human exon 10 with the whole FH gene of the selected species. The resulting nucleotide sequence was considered similar to human exon 10 if the obtained sequence identity score was higher than the lowest sequence identity of the alignment between the respective animal FH sequence human and any human FH exons 2–23 (excluding exon 1, which codes for the secretion signal peptide, which exhibits higher sequence variations, as well as human exon 10, because the comparison is to this exon). Additional requirements for being considered similar to human exon 10 were 1) a splice site consisting of the codons "AG" upstream of the exon start, 2) localization of the found sequence between exon 9 and the exon analog to human exon 11 (i.e., in most cases, exon 10 in the animal sequence), and 3) a nucleotide sequence that codes for maximum 10 aa followed by a stop codon in the correct frame when spliced to the previous exon.

Statistical analysis

All figures show arithmetic mean values with SD of at least three independent assays if not stated otherwise. If representative assays are shown, then the additional repetitions are shown in the supplement. The statistical analyses were performed using the software GraphPad Prism. The details of the statistical tests are given in the respective figure legends. The p values <0.05 were considered to be statistically significant for all tests.

Results

The N-terminal regulatory site of FH exceeds FH domains 1–4 and includes CCPs 5–7

Although FH CCPs 1–4 are sufficient for the complete regulatory functionality of FH, recent data indicated that other domains within the first seven CCPs increase the regulatory activity of the first N-terminal four (31, 36). To identify the CCPs in question and consecutively characterize the functionalities between FH and the extended N-terminal FH regulatory site, we recombinantly expressed a set of FH analytes in the yeast *P. pastoris*, and

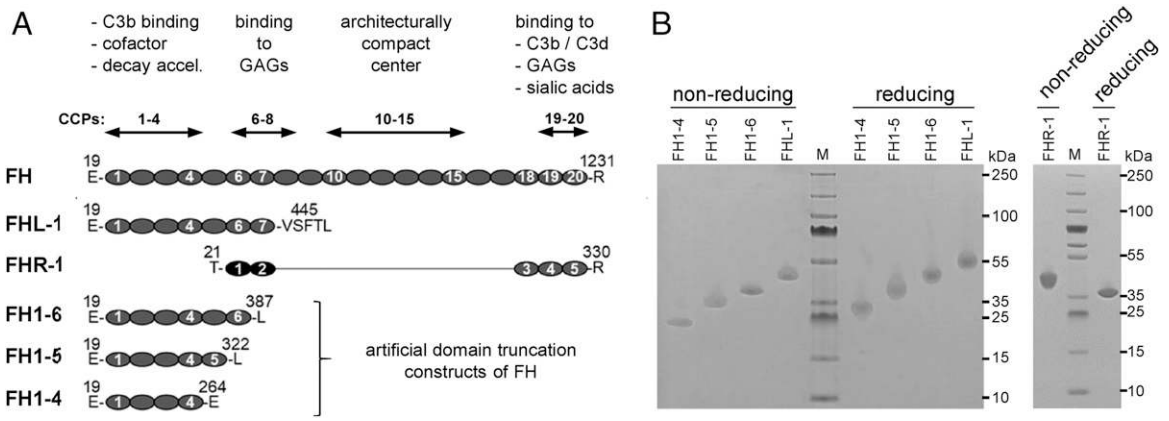

FIGURE 1. Published FH structure–function relationships and SDS-PAGE gel of recombinantly expressed FH protein constructs. (**A**) Schematic representation of the proteins used in this study. Every oval represents a CCP domain of the FH family of proteins as indicated. The first two CCP domains of FHR-1 (shown in black) share 42 and 34% identity with FH CCPs 6 and 7, respectively, whereas the last three domains share 100, 100, and 98% identity to FH CCPs 18–20. Numbers above the amino acids represented in one-letter code indicate the first natural amino acid with numbering including the natural signal peptide sequence of FH or FHR-1, respectively. Domain structure–function relationships of FH domain stretches, as published prior to our study, are indicated at the top. (**B**) SDS-PAGE analysis of recombinantly expressed N-terminal FH truncations and FHR-1. Every lane was loaded with 2 μg total protein under reducing and nonreducing conditions on a 4–12% Bis-Tris gradient gel, which was stained with Coomassie Brilliant Blue R250.

obtained all protein analytes at comparable high quality (Fig. 1B). First, we employed SPR to determine the affinity for C3b. Consistent with published results, FH1-4 and FHL-1 were found to bind C3b with affinities of around 15 and 1.0 μM, respectively (Fig. 2) (7, 33, 37). Extension of FH1-4 by CCP 5 yielded only a small increase in C3b affinity, which is also noticeable by direct comparison of the m.w.-normalized sensorgrams for C3b binding by all analytes at a set concentration of 5 μM (Fig. 2I). Addition of CCP 6 and 6–7 to the construct FH1-5 substantially increased the affinity to 5.5 and 0.9 μM, respectively. Albeit the small effect on C3b affinity upon addition of CCP 5, FH1-5 exhibited, in comparison with FH1-4, increased DAA for C3 convertases (SPR assay) and increased CA for the Factor I–mediated inactivation of C3b in the fluid phase (Fig. 3). Consistent with the higher C3b affinity, FH1-6 and FHL-1 (which correspond to FH1-7) showed higher DAA and CA than FH1-4 or FH1-5. In line with a previous report, FH appears to be a substantially weaker decay accelerator but a considerably better cofactor than the splice variant FHL-1 (or any other N-terminal FH construct tested in this study) (31). The ranking of FH1-4/5/6/7 in isolated DAA and CA assays followed the same overall ranking when the protection from AP-mediated attack of adherent human microvascular endothelial cells (HMEC-1) was probed in FH/FHL-1–depleted serum, confirming the regulatory ranking in a complex and biologically more meaningful environment (Fig. 4A). Collectively, these data demonstrate that the first seven FH domains constitute the full N-terminal regulatory site of FH, even if CCPs 1–4 comprise the minimally required unit for complement regulatory function.

FH is only marginally more active on host cell surfaces than its splice variant FHL-1

In a side-by-side comparison we evaluated FH and its splice variant FHL-1 for their regulatory power to protect different host cell surfaces from complement AP-mediated attack. Apart from fundamental insights into the differential activities of these two regulators within the FH family, the comparison between the extended N-terminal regulatory site within CCP domains 1–7 (i.e., FHL-1) and the full-length protein FH promises to shed light onto the selectivity factor that the FH C-terminus introduces for AP regulation on host cells. A previous study uncovered that FH and FHL-1 exhibit the same protective activity for PNH erythrocytes when diluted human serum is supplemented with either of the two regulators. Because human serum already contains FH and FHL-1, further addition of one of the regulators only changes the relative ratios and hence does not allow a precise determination and comparison of activities. To circumvent this obstacle, we have performed the following assays in commercially available FH-depleted serum, which was demonstrated to be also depleted of FHL-1 (see below) and which is certified to possess full complement functionality. In an equivalent endothelial cell assay as for Fig. 4A, single concentration points or a series of increasing concentrations of FH or FHL-1 were substituted into FH/FHL-1–depleted serum and the mixtures exposed to HMEC-1 with subsequent determination of the level of C3 opsonization. FH exhibited 1.8-fold higher activity in protecting human endothelial cells in comparison with FHL-1 (Fig. 4B, 4C). To test if FH generally is a better regulator on host surfaces, we added FH or FHL-1 to FH/FHL-1–depleted serum and exposed PNH RBCs, which lack two crucial complement regulators and thus are especially susceptible to AP-mediated lysis. Also, on PNH RBCs, FH was more active (1.6-fold) in protecting the host cells in comparison with FHL-1 (Fig. 5, top left panel). Of note, an increase in analytes at lower concentrations leads to higher levels of hemolysis at first before further increase of FH/FHL-1 concentrations protected the RBCs from lysis. This indicates that in FH/FHL-1–depleted serum, a rapid consumption of complement activity takes place in the fluid phase and that only some of the complement activation products from the fluid phase precipitate onto the RBCs' surfaces before all complement components are rapidly consumed without involving a surface. The low concentrations of regulators manage to inhibit complement activation better in the fluid phase than on the erythrocyte surfaces, with this imbalance leading to enhanced RBC lysis, because the regulator concentrations are not yet sufficient to protect the host surfaces. Probably, on erythrocytes this effect is more pronounced than on nucleated cells, because attack by as few as one functional membrane attack complex can be sufficient to lyse a RBC (38), and thus erythrocytes are more sensitive to pick up such a fluid/surface imbalance than nucleated cells.

An activity benefit of FH on host surfaces combined with a penalty for FH regulation on foreign surfaces increases the regulatory selectivity

We hypothesized that FH (IC_{50} of 1.4 μM) would lose its activity benefit over FHL-1 (IC_{50} of 2.2 μM) for protecting RBCs when the host cell marker sialic acid, which is recognized by FH CCP

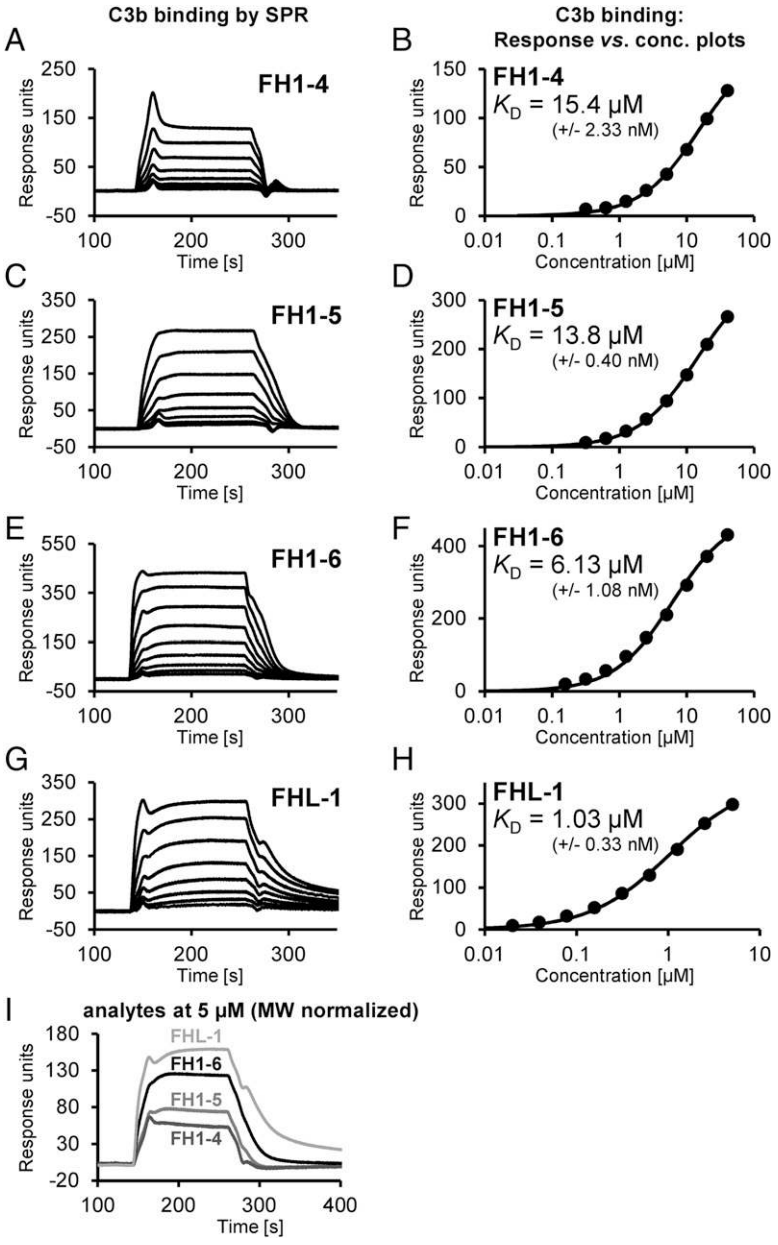

FIGURE 2. C3b binding assessed by SPR. (**A**–**H**) SPR sensorgrams (not normalized to m.w.) of C3b binding and corresponding response–concentration plots with 1:1 steady-state affinity fits as indicated. Recombinant FH constructs were flown over a carboxymethyldextran (CMD) biosensor chip with 3498 RUs (A–D) or 4032 RUs (E–H) of amine-coupled C3b. The corresponding concentration–response plots with the extracted K_D values are shown in the right panels. Reference-subtracted sensorgrams are shown. One out of two (three for FH1–5) SPR analyses is shown (for other SPR assays, see Supplemental Fig. 1). (**I**) Direct comparison of C3b binding of analytes at 5 µM onto amine-coupled C3b (3498 RUs). Reference-substracted sensorgrams were normalized to m.w. to facilitate comparison.

20, was removed (17). This was indeed the case, but rather than falling back to the activity of FHL-1, which exhibits the same activity on normal or desialylated RBCs (IC_{50} of 2.2 µM; Fig. 5, bottom right panel), the FH activity even fell behind the regulatory activity of FHL-1 for desialylated RBCs (IC_{50} of 3.4 µM; bottom left panel), increasing the selectivity factor between host (sialylated human RBCs) and foreign-like (desialylated human RBCs) surfaces from 1.6 to 2.4. To verify that FH indeed receives a regulatory penalty over its complete N-terminal regulatory site of CCPs 1–7 (i.e., FHL-1), we compared the AP-inhibiting activities of the pair FH/FHL-1 on two foreign surfaces. In a hemolytic assay with rabbit RBCs, the addition of increasing amounts of FH and FHL-1 into FH/FHL-1–depleted serum led at first to increased hemolysis, consistent with an imbalance between fluid phase and surface regulation (Fig. 6). When the FH or FHL-1 concentrations were increased further, rabbit RBCs could be protected from AP-mediated lysis, with FHL-1 being ~2-fold more active than FH in inhibiting lysis of the "foreign" rabbit RBCs. Next, we used FH/FHL-1–depleted serum supplemented with FH or FHL-1 and exposed yeast cells to these conditions. Whereas any of the FH concentrations assayed allowed for a robust C3 opsonization of the yeast cells, FHL-1 clearly limited or nearly completely abolished the C3 deposition on this foreign surface (Fig. 7). Thus, the assays with rabbit RBCs and yeast cells confirm that FH receives a regulatory penalty on nonself surfaces when compared with its N-terminal regulatory site of CCPs 1–7.

Because of low serum concentrations, FHL-1 does not contribute substantially to systemic AP control

Because FHL-1 is only ~2-fold less active than FH in protecting PNH RBCs or human microvascular endothelial cells, it is conceivable that FHL-1 contributes substantially to systemic AP control if it reaches serum concentration that are comparable to FH. To quantify the FHL-1 concentration in human serum, we resorted to Western blot analyses of 1) serum samples from healthy donors, 2) FH/FHL-1–depleted serum, and 3) FH/FHL-1–depleted serum substituted with known amounts of FH and FHL-1 as internal standards. Due to the lack of mAbs specific for FHL-1, we used a semiquantitative comparative Western blot analysis, because this allows the detection of FH and its splice variant by

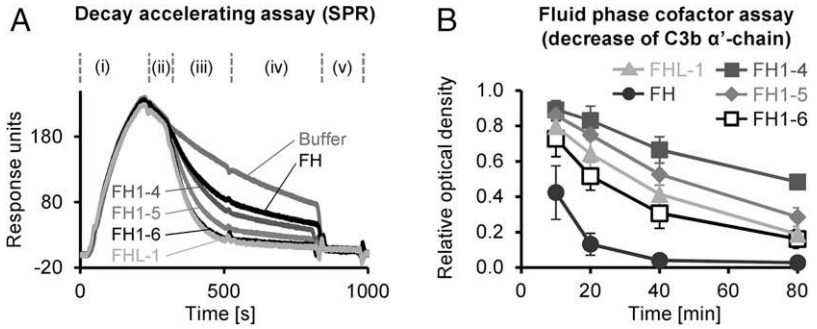

FIGURE 3. Evaluation of decay acceleration and CA of FH N-terminal domain constructs. (**A**) DAA assessed by SPR. AP convertases were built by injecting FB and FD (**i**) onto a carboxymethyldextran (CMD) sensor chip coated with 4918 RU of C3b via standard amine coupling. After monitoring of regular convertase decay (**ii**), FH-derived analytes were injected at 50 nM (**iii**) to evaluate acceleration of the decay rate. Running buffer was flown over the chip for 5 min (**iv**), and the surface was regenerated by injecting CR1 CCPs (1–3) at 0.71 μM (**v**) to decay residual convertases. One out of three independent assays is shown (for other assays, see Supplemental Fig. 1). (**B**) Fluid phase cofactor assay. C3b, Factor I (FI), and one of the analyte proteins were incubated. The generation of iC3b at specific time points (10, 20, 40, and 80 min) was monitored by SDS-PAGE and quantified by densitometry analysis of the disappearance of the band corresponding to the α′-chain (114 kDa) of C3b. Each data point represents the mean of two (FH) or three (FH1-4, FH1-5, FH1-6, FHL-1) independent assays with SD shown, respectively (for SDS-PAGE gels of this analysis, see Supplemental Fig. 2). Statistical analysis was performed using two-way ANOVA with Tukey multiple comparisons test: the time courses of the CA of all analytes were compared with each other; the activity of FH was significantly better than the activities of any other construct. The activity of FH1-6 was significantly better than the activity of FH1-4. The differences in activities for all other comparisons were statistically not significant.

the same mAb on the same blot due to separation of the two proteins by size. By comparing the band intensities of the donors' samples and the NHS serum pool with the ones of the internal standards, it is apparent that the FH concentrations of the NHS pool and of donors 1 and 2 are between 1.7–3.3 μM, with the serum of donor 3 containing less FH (between 0.8 and 1.7 μM) (Fig. 8). The same comparison for the FHL-1 bands indicates that in the tested sera, FHL-1 is present at a concentration of ∼0.04 μM, resulting in a molar FH to FHL-1 ratio of ∼40:1. With this ratio it is not plausible that FHL-1 plays a substantial role for systemic AP control. Apart from differential systemic expression levels, also, differences in pharmacokinetic plasma clearance could account for

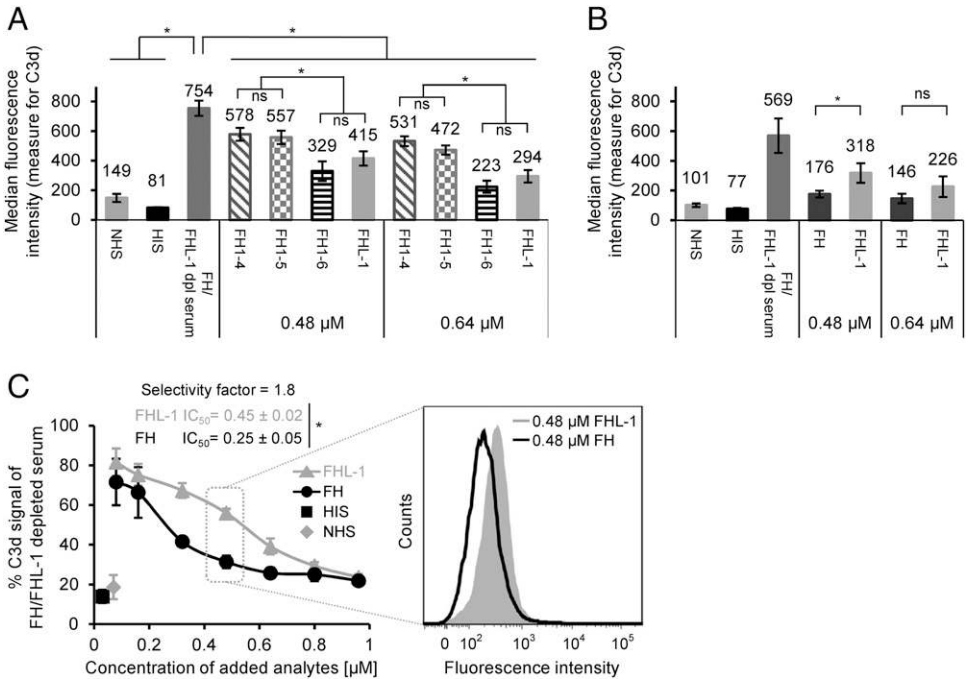

FIGURE 4. Protection of human endothelial cells from C3 opsonization by FH analytes. (**A**) Adherent human microvascular endothelial cells (HMEC-1) were exposed to FH/FHL-1–depleted serum substituted with FH analytes (final serum content 40%) or control reactions. The cells were incubated with FH analytes at either 0.48 or 0.64 μM. After trypsinization, the amount (median fluorescence intensity [MFI]) of C3d (which is trypsin resistant) was determined by flow cytometry as a measure of C3 opsonization. The mean of the MFI of three independent assays with SD is shown (for primary flow cytometry data, see Supplemental Fig. 3A). Statistical analysis was performed using one-way ANOVA with Tukey multiple comparisons test. An asterisk (*) denotes significance. (**B**) Same as in (A), but here FH or FHL-1 was added to FH/FHL-1–depleted serum and exposed to the cells. The mean of the MFI of three independent assays with SD is shown. (**C**) Same as in (A) and (B), but here a concentration series of FH or FHL-1 was added to the cells. On the right side, an exemplary histogram is shown (for all primary data, see Supplemental Fig. 3B). The mean MFI of three independent assays with SD is shown (except for the FH and FHL-1 data points at a concentration of 0.08 μM, which were only assayed twice). IC_{50} values are mean values of three independent experiments with SD. For glycine buffer control in this endothelial cell assay, see Fig. 10. Statistical analyses were performed using the unpaired *t* test (two-tailed). An asterisk (*) denotes significance. HIS, heat-inactivated serum; ns, not significant.

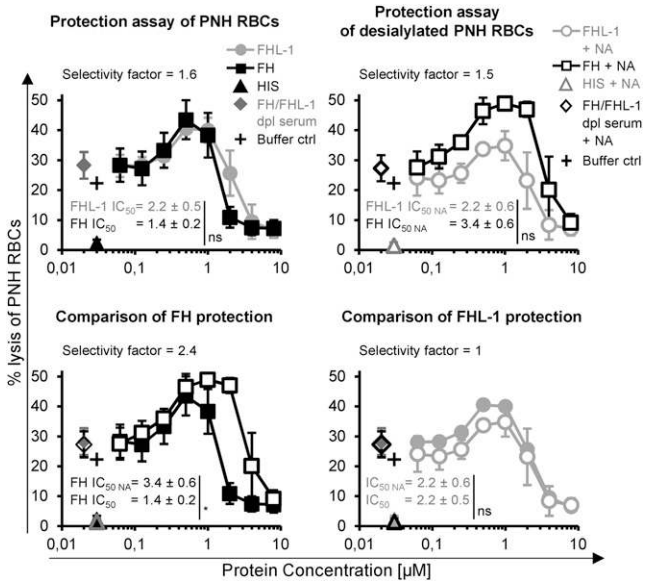

FIGURE 5. Protection of PNH erythrocytes from lysis by FH and FHL-1. Lysis of PNH RBCs, mediated by AP activation, was measured in FH/FHL-1–depleted serum (40% final serum content, supplemented with EGTA), which was spiked with analytes as indicated. PNH RBCs were also probed and desialylated after treatment with neuraminidase before exposure to serum. Release of hemoglobin as an indicator of lysis was measured by determining UV absorbance at 405 nm and set in relation to complete lysis in H_2O. NHS contained the same amount of PBS as the FH/FHL-1–depleted serum contained by adding of the analytes (in PBS) into the serum. In analogy, the buffer control contained the same amount of FHL-1 buffer (i.e., glycine buffer) as the sample with the highest FHL-1 concentration to exclude any influence mediated by the different buffer. To facilitate data interpretation, each curve is displayed twice within a different group. The IC_{50} and $IC_{50\ NA}$ values are calculated on the basis of the five highest concentration points. Selectivity factor is the quotient of the lower IC_{50} (or $IC_{50\ NA}$) to the higher IC_{50} (or $IC_{50\ NA}$). Data points are mean values of three independent experiments with SD. IC_{50} values are mean values of three independent experiments with SD. Statistical analyses were performed using the unpaired *t* test (two-tailed). An asterisk (*) denotes significance. HIS, heat-inactivated serum; IC_{50}, half maximal inhibitory concentration; $IC_{50\ NA}$, half maximal inhibitory concentration for cells treated with Neuraminidase; NA, neuraminidase; ns, not significant.

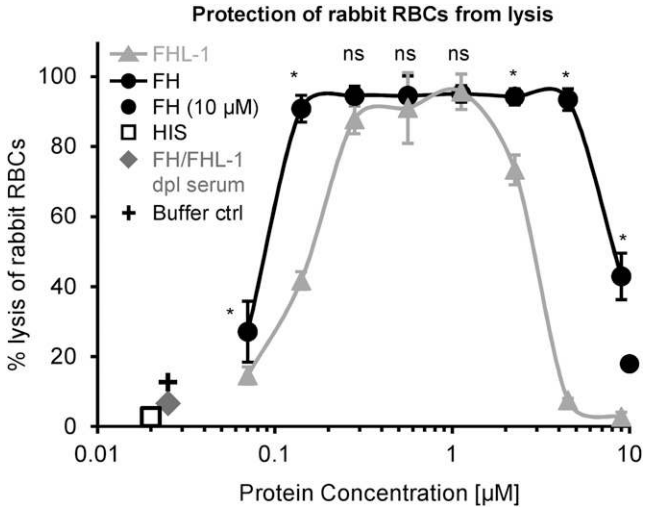

FIGURE 6. Protection of rabbit erythrocytes by FH and FHL-1. FH or FHL-1 was mixed with FH/FHL-1–depleted serum (40% final serum content) and rabbit erythrocytes. Lysis was measured indirectly by quantification of released hemoglobin (measured at 405 nm). All values were normalized to lysis in H_2O. Data points are the mean of three independent assays with SD. FH at 10 μM was only assayed once as technical duplicate. Statistical analysis was performed using two-way ANOVA with Sidak multiple comparisons test. An asterisk (*) denotes significance. HIS, heat-inactivated serum; ns, not significant.

the high serum ratio between FH and its splice product. To this end we determined the terminal plasma half-life time (β-phase $T_{1/2}$) by injecting the human proteins into mice. With a β-phase $T_{1/2}$ of 18.3 and 2.9 h for FH and FHL-1 in mice, respectively, FHL-1 exhibits a 6-fold higher murine plasma clearance rate than its parent molecule FH (Fig. 9).

FHL-1 resists deregulation by FHR-1 and occurs late in evolution

The low availability in serum and the fast plasma clearance of FHL-1 indicate that the main purpose is not the systemic but rather the local control of the AP. We hypothesized that the lack of 13 C-terminal domains may confer one potential regulatory advantage over FH: due to the lack of C-terminal FH domains 19–20 (which are highly homologous to the C-terminal domains of FHRs), FHL-1 may resist deregulation by FHRs, which is a mechanism by which FHR molecules compete FH off surfaces with extra high loads of C3b to allow AP attack on these supposedly dangerous surfaces (39–41) (reviewed in Ref. 42). First, we tested the level of FH deregulation on endothelial cells by adding different amounts of recombinantly expressed FHR-1 (dimer) to 40% NHS (Fig. 10A), with the lowest and highest recombinant FHR-1:FH ratio being 0.23 and 7.5, respectively. Physiological FHR-1:FH ratios were reported to be in the range of 0.4–0.8 (43) or lower (44). Even the addition of such moderate concentrations of recombinant FHR-1 dimers to NHS (already containing natural FHR molecules) led to noticeable but small increases in C3b deposition. However, C3b deposition increased proportionally with further addition of unnaturally high amounts of FHR-1. As described above, C3 opsonization was determined by flow cytometry as a measure for AP activation on endothelial cells. We then investigated the competition between FH or FHL-1 and the most abundant FHR protein (i.e., FHR-1) in the defined system of FH/FHL-1–depleted serum being supplemented with either FH or FHL-1 before being exposed to endothelial cells (Fig. 10B). The high concentration of 9.6 μM of FHR-1 dimer in this assay was chosen to account for the high natural FHR-1 to FHL-1 ratio, because we have shown above that the systemic FHL-1 concentration is only about one fortieth of the FH plasma concentration. Whereas addition of FHR-1 to FH containing serum led to dramatic increases in C3 opsonization, addition to FHL-1 containing serum led to a comparatively small increase in C3 opsonization (Fig. 10B), demonstrating that FHL-1 considerably resists the deregulation by FHR-1. Another indication for a specialized role of FHL-1 is its late occurrence in evolution. In silico gene analysis revealed that high homology to the human FH exon 10 (which is responsible for the alternative splice product FHL-1) is only found in the order Catarrhini (old-world monkeys) (Tables I, II). Although it cannot be ruled out that alternative splicing also occurs in Platyrrhini (new-world monkeys), the resulting gene products of the investigated species could differ considerably, and the lack of the nonobligate splice acceptor site indicates that splicing is unlikely to occur. For *Callithrix jacchus* (common marmoset), an exon with poor homology to the human FH exon 10 has been identified that would encode for a rather similar short peptide stretch. However, because this exon is located between exons 13 and 14 (corresponding to human FH exons 14 and 15), the splice variant in this species would comprise the first 11 CCP domains instead of the first seven, as seen in Catarrhini. For *Saimiri boliviensis* (black-capped squirrel monkey), the potential splice variant would end after CCP domain 7, with the potential peptide stretch spanning 10 unique amino acids. Despite of its low sequence

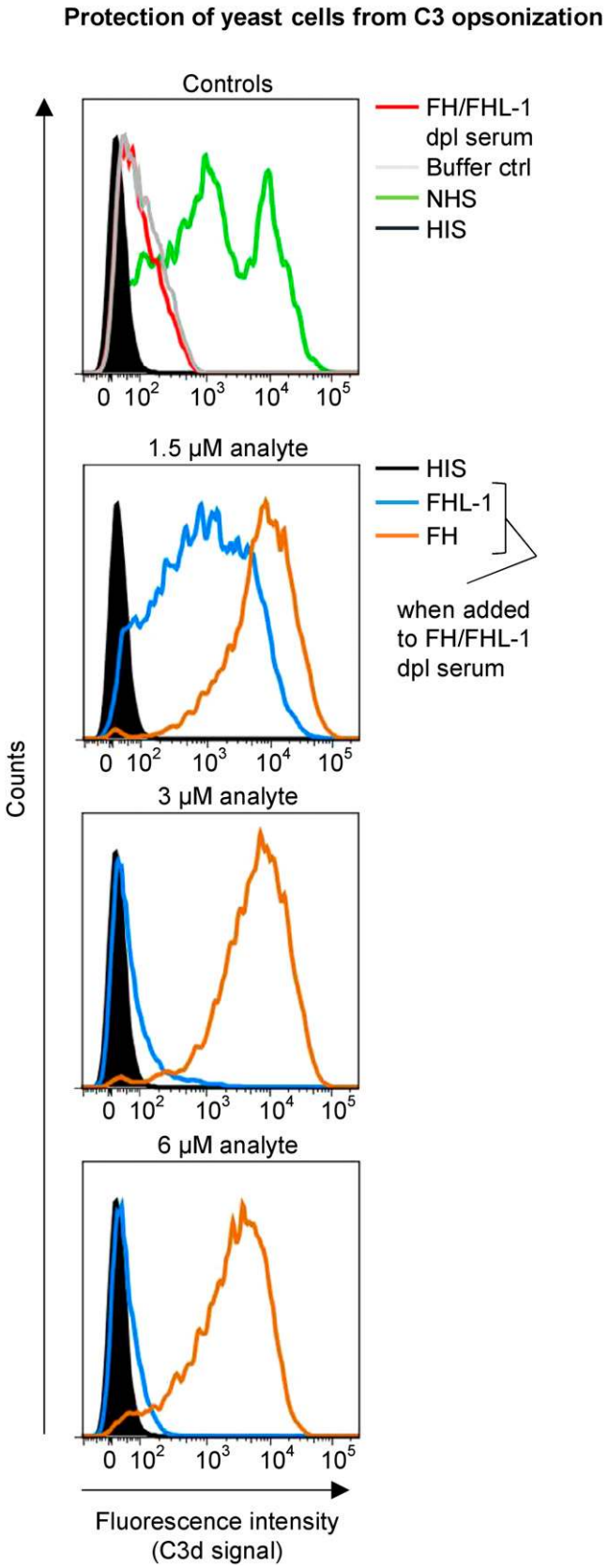

FIGURE 7. Protection of yeast cells from C3 opsonization by FH analytes. Cells of the yeast *P. pastoris* were exposed to FH/FHL-1–depleted serum supplemented with analytes (40% final serum content, supplemented with EGTA). Afterwards, yeast cells were analyzed for anti-C3d labeling by flow cytometry as a measure of C3 opsonization. One of four representative assays is shown (for the other three assays, see Supplemental Fig. 3C). Heat-inactivated serum (HIS) is identical in all four panels. The buffer control contains as much FHL-1 buffer as FHL-1 in the highest concentrated sample. Controls are represented in the upper panel, whereas the lower three panels show the analytes at 1.5, 3, and 6 µM when those were added to FH/FHL-1–depleted serum.

homology to the human splicing exon 10 and the missing splice acceptor site "AG," if produced, the splice variant in this species would be rather similar to the human FHL-1 protein. The only other investigated sequence in this order *Aotus nancymaae* (Nancy Ma's night monkey) is also lacking the not-obligate splice acceptor site AG, and, if produced, would again be similar to human FHL-1 protein. Although it is known that mice do not express a FH splice variant (45), further in silico gene analyses of primates in the orders Lemuriformes and Lorisiformes identified only poorly homologous sequences that lie within the first four exons, ruling out that those hits can produce regulatory active splice variants.

Discussion

This study compares FH and its splice variant FHL-1 in terms of their potency to protect human host or foreign cell surfaces from an attack by the AP. FH is only 1.6- to 1.8-fold more active in protecting the host surfaces of patient-derived PNH RBCs or human endothelial cells. Considering that FHL-1 lacks the key self versus nonself discriminator in FH (i.e., CCPs 19–20), the rather high regulatory activity for FHL-1 is remarkable and at first sight implies a very narrow selectivity gain for FH introduced by its C-terminus. We found that the N-terminal regulatory site of CCPs 1–4 in FH extends and includes CCPs 5–7, providing a rationale as to why FHL-1 and FH are more similar in their activities than anticipated. Although there is only a small contribution of CCP 5 to C3b binding, extension by CCPs 5–7 boosts the affinity of FH1-4 for C3b ~15-fold. This is in line with previous data showing that FH CCPs 6–8 and 7–8, but not 8–9, show a weak binding response to C3b (7). Even though C3b binding strength is only marginally increased by adding CCP 5 to FH1-4, every functional assay showed improved regulatory activity of FH1-5 over FH1-4. Further extension by domains 6 and 7 improved C3b binding, CA, and DAA and resulted in better overall complement regulation in serum. Whereas addition of CCP 7 to FH1-6 had the highest effect in increasing affinity for C3b, the addition of CCP 6 to FH1-5 produced the biggest regulatory gain in all complement functional assays. In the endothelial cell protection assay, there was only a small regulatory difference between FH1–6 and FH1–7 (FHL-1), showing overall comparable activity. This finding confirms the previous notion that the increase in affinity for the target C3b above a certain threshold may not necessarily lead to higher regulatory activity. Apart from target binding (i.e., C3bBb or C3b), also target release (i.e., C3b or iC3b, respectively) and thus the turnover rate of a regulator substantiates the overall regulatory activity (31). One earlier report had found a high activity difference between FH and FHL-1 when DAA on sheep erythrocytes had been assayed in absence of serum (46), but our latest findings in this study as well as our own previous findings support the high regulatory activity of FHL-1 toward the AP (31), indicating that the discrepancies may arise from the specialized DAA assay performed in the previous study (46). Additional indirect support for FHL-1 exhibiting substantial regulatory activity toward the AP comes from the fact that certain pathogens like the spirochete *Borrelia spielmanii* (i.e., bacteria causing Lyme disease) preferentially recruit FHL-1 for immune evasion (47).

The distinction between FH and FHL-1 is not only the absence of the key functional site within CCPs 19–20 but also the lack of the entire middle domains of FH. To determine the selectivity

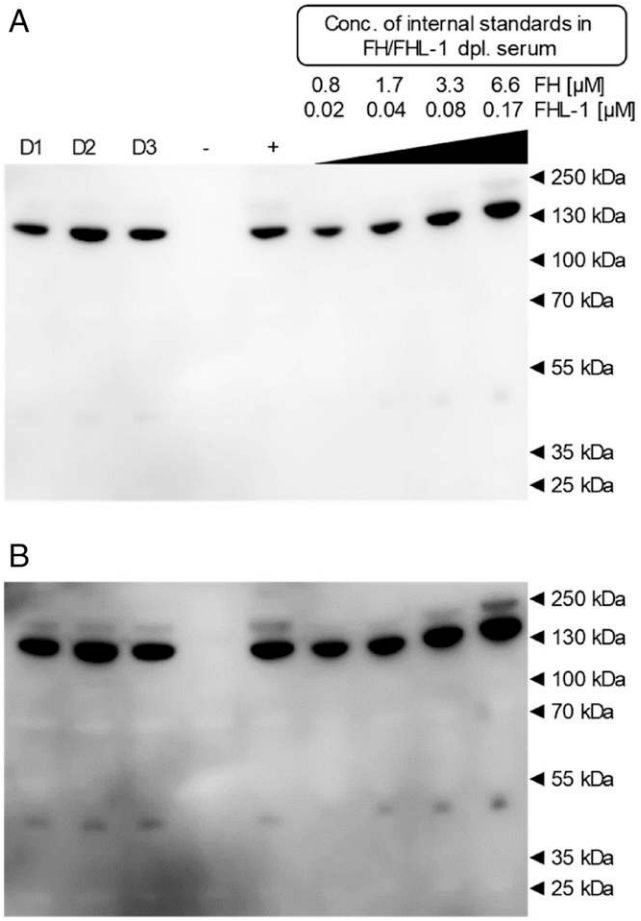

FIGURE 8. Western blot analysis of FH/FHL-1 concentrations in serum. Diluted human serum (3.75% final serum content per lane) was separated on a 4–12% Bis-Tris gradient SDS-PAGE gel and transferred to a PVDF membrane. Proteins were detected with an anti-human FH Ab that binds to CCP1. (**A**) The membrane was exposed for a short period to distinguish the intensity of FH bands (155 kDa). (**B**) After longer exposure, FHL-1 appears at 49.3 kDa. Serum of healthy donors is shown in lanes D1, D2, and D3. FH/FHL-1–depleted serum was loaded on lane "−" and commercially available pooled NHS is shown in lane "+." The last four samples consist of FH/FHL-1–depleted serum that was supplemented with increasing concentrations of purified FH and FHL-1 to allow semiquantitative analysis by comparison. One representative blot of three is shown (for other two blots, see Supplemental Fig. 4).

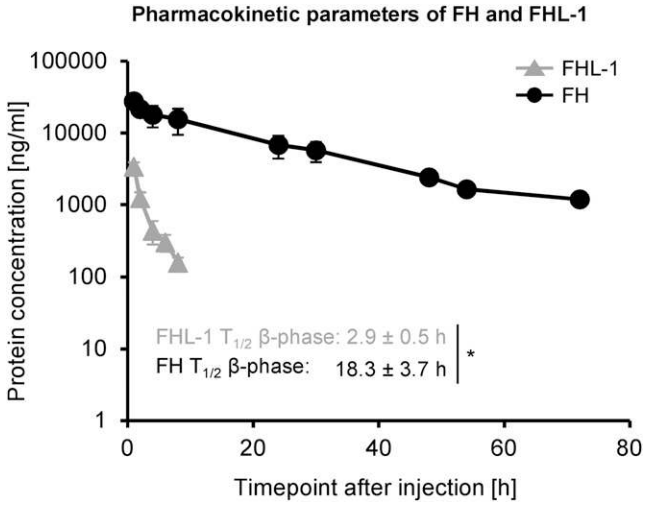

FIGURE 9. Determination of pharmacokinetic parameters of FH and FHL-1 in mice. A single dose of FH (100 μg) or FHL-1 (60 μg) was injected i.v. into male C57BL/6 mice (n = 4 each group). At various time points, blood samples were taken and plasma concentrations were determined with a sandwich ELISA. Mice were sacrificed after 8 or 72 h. Data points show the mean values with SD. The values for the β-phase plasma half-life time are mean values of individual half-life times within each group with SD. Statistical analysis was performed using the unpaired t test (two-tailed). An asterisk (*) denotes significance.

difference between FH and its splice variant and thus to establish the specificity factor of FH for host over foreign surfaces, FH and FHL-1 (both containing the extended N terminus) were compared for their capacity to protect several self and nonself surfaces. In the PNH RBC protection assay, FH was moderately (1.6-fold) more active than FHL-1. This activity benefit for FH is likely caused by the presence of sialic acids on the surface of RBCs, which are recognized by the FH C-terminus (CCP 20), whereas FHL-1 does not bind sialic acids, as has been shown recently (12). By removing the erythroid host selectivity marker sialic acid with neuraminidase, we aimed at converting a host cell surface into one that resembles a nonself one. As expected, the regulatory activity of FHL-1 was not affected by desialylation. In contrast, the activity of FH to protect desialylated PNH RBCs did not only fall back to the activity of FHL-1, which would be consistent with the interpretation that FH simply loses the regulatory benefit introduced via the sialic acids. On desialylated PNH RBCs, FH was even less active than FHL-1 (1.5-fold), implying that, in absence of sialic acids, the first seven domains within FH experience a regulatory penalty compared with FHL-1. By comparing the activities of FH for sialylated and desialylated PNH RBCs directly, both sialic acid–dependent mechanisms of FH are accounted for: the regulatory benefit as well as the regulatory penalty. Thus, the selectivity factor introduced by sialic acids for FH in protecting (in serum) self or nonself is ∼2.4. This finding is consistent with previous studies that reported increased binding by FH when C3b-coated surfaces also contained sialic acids (48–50). To substantiate that CCPs 1–7 within FH indeed experience a regulatory penalty over FHL-1 on nonself surfaces, comparisons on two more foreign cell types were performed. Compared with FH, FHL-1 protected rabbit RBCs and yeast cells substantially better from complement attack. Mechanistically, we propose that a closed conformation of FH impairs FH functionality and thus is responsible for the regulatory penalty of FH in absence of sialic acids. The lack of sialic acids means that FH loses 1) a binding partner and thus avidity for C3b and sialic acid on the surface to be protected, and 2) a key to unlock the less active, closed FH conformation that keeps both FH termini packed against each other, thus mutually impairing their accessibility. This notion is supported by the discovery that FH is folded back upon itself (51), the proposal that FH has a compact conformation that may be altered (52), the discovery that the central FH domains 10–15 have a compact structure that extends in FHΔ10–15 upon deletion of the domains 10–15 (31, 53), that direct connection of the FH N-terminal and C-terminal functional sites (i.e., versions of miniFH) yields substantial higher regulatory activity (30, 36, 54), that cross-links between CCP 4 and 20 are detected in FH (55), and that the bacterial protein PspC transforms FH from a latent into a functionally enhanced form (55).

Apart from the insights into the selectivity of FH regulation introduced by the host marker sialic acid, our study has established that FHL-1 is almost as active as FH in regulating the AP. However, because FHL-1 fails to effectively distinguish between several host and foreign surfaces when compared with FH, it is doubtful that substantial amounts of FHL-1 in the systemic circulation would be of benefit to the host. Although FHL-1 can actively regulate the

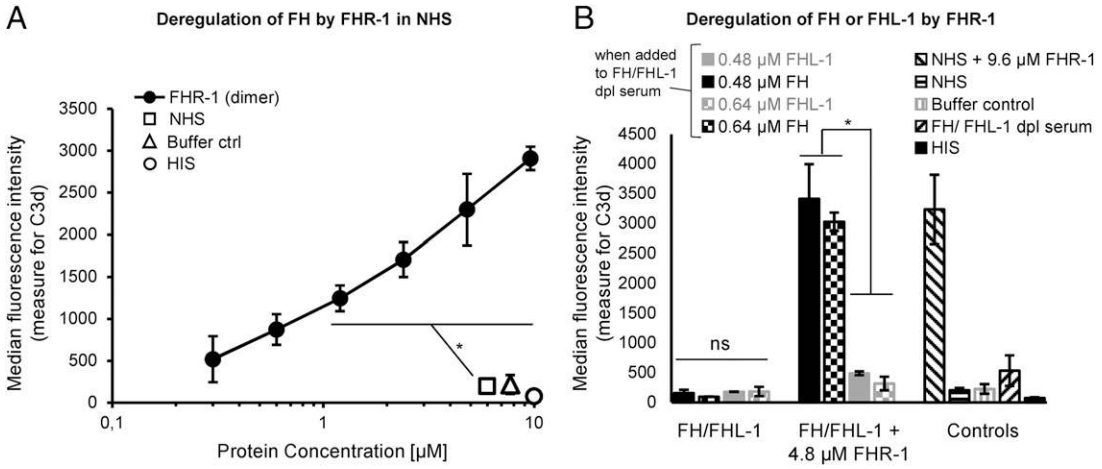

FIGURE 10. C3 opsonization mediated by FHR-1 deregulation. (**A**) Endothelial cells (HMEC-1) were incubated with NHS in presence of increasing amounts of recombinant FHR-1 (dimer). Identical to previous endothelial cell assays, cells were labeled with anti-C3d Ab to measure levels of C3 opsonization. Mean values of two independent assays with SD are shown. Statistical analysis was performed using one-way ANOVA with Dunnett multiple comparisons test. (**B**) As in (A), but this time endothelial cells (HMEC-1) were incubated with FH/FHL-1–depleted serum in presence of one of the analytes and FHR-1 where stated. The ratio of FHR-1 (dimer) to FH/FHL-1 was 20 at an analyte concentration of 0.48 μM, 15 at an analyte concentration of 0.64 μM, or 7.5 in NHS (assuming an FH concentration of ~1.28 μM in 40% serum), with 9.6 μM FHR-1. For 0.48 μM FH and 0.64 μM FHL-1 with or without FHR-1 and all controls, mean values of three independent assays with SD are shown. All others (0.64 μM FH $^{+/-}$ FHR-1, 0.48 μM FHL-1 $^{+/-}$ FHR-1) show mean values of one assay with three technical replicates. Statistical analyses were performed using one-way ANOVA with Tukey multiple comparisons test where appropriate. An asterisk (*) denotes significance. ns, not significant.

AP, high systemic FHL-1 concentrations could be hazardous to the host as FHL-1 protects self and nonself surfaces similarly well. An exploratory study using a subtraction method after double and single detection of FH and FHL-1 or FH only, respectively, found the molar ratio between FH and FHL-1 in the circulation to be ~2:1 (6, 56). To avoid indirect measurements, we resorted to a direct but semiquantitative determination method using SDS-PAGE separation and Western blot detection of FH and FHL-1 using the same mAb and comparing the band intensities to an internal standard curve. This has revealed that the molar FHL-1 concentration in humans is only about one fortieth of the one of FH. Apart from differences in expression levels (which have not been analyzed in this article), differential plasma clearance rates could also be responsible for the low systemic FHL-1 concentrations and thus protect the host from introducing unselective AP control in the systemic compartment. To test if this hypothesis is true, we determined the terminal plasma half-lifetime of human FH and FHL-1 when i.v. injected into mice. Human FHL-1 was cleared ~6-fold faster from the murine circulation than FH, indicating that FHL-1, indeed, is also subject to higher plasma clearance in humans.

These insights into the FHL-1 biology raise the question of what biological benefits were introduced by producing the splice variant FHL-1. Because, in humans, FHL-1 circulates at a low concentration in plasma, it is feasible that FHL-1 has a particular role in controlling the AP in local tissues. Indeed, it has been shown recently that retinal pigment epithelial cells predominantly express FHL-1 instead of FH (57). These results implied that FHL-1 is the predominant AP regulator within the Bruch membrane, the layer of extra cellular matrix that is known to be a major site for the disease pathogenesis of AMD. Other studies have also observed that certain cell types (e.g., fibroblasts) express the splice version, further supporting the notion of a specialized role for FHL-1 outside the systemic compartment (58). Several cancer tissues/cell lines were shown to specifically upregulate the expression of the splice variant FHL-1, which in this occasion appears detrimental to the organism due to cancer cells trying to protect themselves unspecifically from complement attack. Examples are human astroglioma cell lines (59), glioblastoma (60), and ovarian tumor cells (61). Potential physiological reasons (or in the case of upregulation by malignant cells, pathophysiological reasons) for upregulated FHL-1 expression may be that 1) FHL-1 is sufficient to provide good AP regulation without the need to produce the other 13 CCP domains, 2) FHL-1 has higher tissue penetrability in comparison with FH (57, 62), and/or 3) because FHL-1 lacks the FH C-terminal domains, it may be less susceptible to deregulation by FHR proteins, and therefore FHL-1 might be a better AP regulator than FH on tissues that also express or have access to substantial levels of FHR proteins. We tested this hypothesis on human endothelial cells exposed to FH/FHL-1–depleted serum that had been substituted with FH or FHL-1 and the most common FHR protein in human plasma, FHR-1 (Fig. 10B). Although some degree of deregulation of FHL-1 by FHR-1 is apparent, the comparison with FH demonstrates that FHL-1 substantially resists deregulation, thus supporting the hypothesis that FHL-1 may indeed be a more potent regulator in local tissues known to produce FHR proteins. In silico gene analysis revealed that our nearest relatives in the order of old-world monkeys have gene structures that support production of FH splice variants identical or very similar to the human FHL-1 protein, whereas splice variants are less likely to appear throughout the order of new-world monkeys, and if they occur, they can differ considerably from the human version. For two other primates outside the orders of old- or new-world monkeys, no indication for an alternatively splicing exon that produces a product like FHL-1 has been found. Taken together, the finding that FHL-1 is the major regulator in the Bruch membrane, that FHL-1 considerably resists deregulation by FHR proteins, and that it occurs relatively late in evolution argue that FHL-1 has a particular role in controlling the AP at local sites. It will be useful for future studies to confirm the late phylogenetic occurrence at protein level and potentially identify the underlying, relatively young and specific biological function(s) that facilitated the development of FHL-1 expression.

Our findings provide important insights into how the major AP regulator FH achieves selectivity for host surfaces. By employing a two-sided discriminatory mechanism, FH increases its selectivity factor to be more specific for the protection of self surfaces: whereas

Table I. Sequence identities between FH exons from human and nonhuman primates

		Sequence Identity to Human FH Exons in % (Exon Number According to Human FH Gene); in Parentheses: (Sequence Identity of Coding Amino Acid)																						
Order	Species	1	2	3	4	5	6	7	8	9	10	11	12	13	14	15	16	17	18	19	20	21	22	23
Catarrhini (old-world monkeys)	*Homo sapiens* (human)	100 (100)	100 (100)	100 (100)	100 (100)	100 (100)	100 (100)	100 (100)	100 (100)	100 (100)	100 (100)	100 (100)	100 (100)	100 (100)	100 (100)	100 (100)	100 (100)	100 (100)	100 (100)	100 (100)	100 (100)	100 (100)	100 (100)	100 (100)
	Pan troglodytes (common chimpanzee)	98 (100)	98 (97)	98 (100)	100 (100)	100 (98)	99 (98)	98 (95)	97 (94)	98 (95)	99 (100)	100 (100)	100 (100)	100 (100)	99 (98)	98 (100)	100 (100)	98 (97)	100 (98)	100 (100)	99 (98)	99 (100)	94 (97)	95 (84)
	Pongo abelii (sumatran orangutan)	98 (100)	98 (98)	96 (94)	100 (100)	95 (91)	97 (95)	97 (95)	95 (86)	95 (92)	98 (75)	96 (93)	96 (88)	98 (97)	97 (95)	97 (97)	91 (78)	100 (100)	98 (98)	97 (95)	98 (93)	96 (95)	100 (100)	94 (87)
	Papio anubis (olive baboon)	95 (95)	94 (87)	94 (91)	100 (100)	94 (84)	98 (95)	93 (85)	93 (88)	92 (80)	95 (50)	95 (89)	94 (86)	94 (92)	96 (92)	95 (93)	87 (68)	95 (90)	96 (94)	96 (93)	94 (90)	93 (86)	96 (92)	87 (68)
	Macaca fascicularis (cynomolgus monkey)	94 (95)	95 (89)	94 (91)	100 (100)	93 (81)	97 (93)	94 (90)	94 (91)	93 (83)	95 (50)	95 (89)	94 (86)	94 (92)	96 (95)	94 (93)	88 (70)	96 (92)	96 (94)	97 (95)	94 (90)	94 (88)	96 (92)	88 (69)

		Sequence Identity to Human FH Exons in % (Exon Number in Order of Appearance, but Columns Are Aligned to Corresponding Human FH Exons Above)																					
Order	Species	1	2	3	4	5	6	7	8	9	10	11	12	13	14	15	16	17	18	19	20	21	22
Platyrrhini (new-world monkeys)	*S. boliviensis* (black-capped squirrel monkey)	88 (74)	90 (81)	87 (77)	95 (89)	90 (80)	89 (81)	84 (70)	81 (60)	85 (66)	87 (77)	90 (81)	90 (83)	92 (87)	91 (88)	87 (76)	90 (89)	91 (86)	90 (83)	85 (71)	81 (68)	93 (90)	81 (59)
	A. nancymaae (nancy ma's night monkey)	91 (90)	90 (86)	88 (80)	96 (96)	90 (81)	91 (81)	87 (76)	87 (75)	86 (66)	92 (84)	89 (76)	90 (83)	92 (87)	91 (87)	85 (73)	93 (89)	91 (84)	89 (83)	84 (75)	89 (80)	93 (92)	80 (55)
	C. jacchus (common marmoset)	90 (84)	89 (84)	87 (77)	96 (96)	90 (77)	92 (88)	91 (83)	89 (79)	86 (66)	90 (80)	89 (80)	92 (85)	92 (87)	92 (88)	83 (66)	92 (90)	91 (82)	90 (81)	88 (75)	81 (73)	93 (92)	74 (52)
Lemuriformes	*Propithecus coquereli* (coquerel's sifaka)	82 (68)	86 (71)	87 (77)	95 (85)	82 (69)	87 (74)	89 (74)	76 (65)	77 (58)	87 (74)	78 (64)	85 (73)	87 (79)	83 (80)	76 (63)	91 (85)	74 (64)	79 (72)	79 (61)	84 (71)	85 (77)	50 (52)
Lorisiformes	*Otolemur garnettii* (northern greater galago)	81 (63)	85 (74)	86 (80)	87 (62)	80 (63)	83 (70)	80 (72)	78 (63)	77 (53)	83 (66)	79 (66)	85 (70)	84 (72)	86 (73)	73 (53)	86 (74)	75 (70)	81 (66)	72 (51)	80 (70)	88 (87)	66 (57)
Rodentia	*Mus musculus* (house mouse)	54 (32)	79 (66)	70 (66)	84 (81)	80 (70)	65 (60)	72 (62)	71 (54)	70 (53)	54 (62)	74 (64)	71 (54)	78 (69)	77 (72)	61 (46)	77 (61)	72 (63)	70 (62)	62 (53)	73 (59)	81 (79)	57 (46)
	Rattus norvegicus (brown rat)	62 (68)	79 (65)	76 (71)	87 (92)	80 (7)	74 (68)	75 (69)	76 (68)	65 (48)	76 (67)	72 (68)	68 (49)	77 (64)	71 (67)	70 (49)	70 (59)	70 (65)	73 (66)	65 (53)	76 (64)	81 (80)	57 (49)

Table II. Alignment characteristics when human FH exon 10 (coding for FHL-1) was aligned to FH genes of diverse animals

Order	Species	Sequence Identity (%) of Human Exon 10 Queried on the Whole Animal FH Gene, Nucleotide (Amino Acids)	Lowest Sequence Identity When Animal FH Sequences Were Aligned onto Human FH Exons 2–9 or 11–23 (Each at a Time); Excluding Exon 1 (Secretion Signal) and Human Exon 10 (Alternate Splicing Site)	Splice Site ("AG") Upstream of Found Query Sequence	Localization between Exon 9 and the Exon Corresponding to Human Exon 11	Sequence Coding for Maximum 10 aa Followed by a Stop Codon (aa Sequence)
Catarrhini (old-world monkeys)	*H. sapiens* (human)	**100 (100)**	100	+	+	+ (SFTL)
	P. troglodytes (common chimpanzee)	**99 (100)**	94	+	+	+ (SFTL)
	P. abelii (sumatran orangutan)	**98 (75)**	91	+	+	+ (SFTH)
	P. anubis (olive baboon)	**95 (50)**	87	+	+	+ (RFTH)
	M. fascicularis (cynomolgus monkey)	**95 (50)**	88	+	+	+ (RFTH)
Platyrrhini (new-world monkeys)	*S. boliviensis* (black-capped squirrel monkey)	52 (30)	81	–	+	+ (NFTLHAGPIL)
	A. nancymaae (Nancy Ma's night monkey)	53 (0)	80	–	+	+ (R)
	C. jacchus (common marmoset)	37 (50)	74	+	Between exons 13 and 14, which correspond to human exons 14 and 15	+ (GCTL)
Lemuriformes	*P. coquereli* (coquerel's sifaka)	39 (—)	50	–	Between exons 3 and 4	–
Lorisiformes	*O. garnetti* (northern greater galago)	40 (—)	66	–	Between exons 1 and 2	+ (GLTVFGVYEDF)
Rodentia	*M. musculus* (house mouse)	42 (—)	57	–	+	–
	R. norvegicus (brown rat)	39 (—)	57	–	Between exons 5 and 6	–

Bold font indicates that the alignment of an animal FH gene to the human exon 10 resulted in a higher sequence identity than was achieved for the alignments to at least one of the other probed human exons (i.e., 2–9 or 11–23). Underlined numbers indicate that the alignment of the animal FH gene to human FH exon 10 resulted in the lowest sequence identity among all other probed human exons (i.e., 2–9 or 11–23). The "+" or "–" symbols in the table body denote that the column heading applies or does not apply, respectively.

FH experiences gain in activity on sialic acid–bearing surfaces, when compared with its stand-alone N-terminal regulatory site within FHL-1, on surfaces lacking sialic acids, FH receives a regulatory penalty. Moreover, we have uncovered that the N-terminal functional site of FH spans the CCP domains 1–7 and that FHL-1 is a much more active complement regulator than known to date. We suggest that, because of its differential functionality (e.g., its fast plasma clearance and its resistance to be deregulated by FHR proteins) and its evolutionary late occurrence, FHL-1 is especially poised to be an efficient regulator on specialized local tissues. This notion supports the concept that the AMD pathophysiology in respect to the AMD-associated FH polymorphism (Y402H) is driven by the splice variant FHL-1 rather than the parent molecule FH (57).

Disclosures

The authors have no financial conflicts of interest.

References

1. Ricklin, D., G. Hajishengallis, K. Yang, and J. D. Lambris. 2010. Complement: a key system for immune surveillance and homeostasis. *Nat. Immunol.* 11: 785–797.
2. Pangburn, M. K., R. D. Schreiber, and H. J. Müller-Eberhard. 1981. Formation of the initial C3 convertase of the alternative complement pathway. Acquisition of C3b-like activities by spontaneous hydrolysis of the putative thioester in native C3. *J. Exp. Med.* 154: 856–867.
3. Gros, P., F. J. Milder, and B. J. C. Janssen. 2008. Complement driven by conformational changes. *Nat. Rev. Immunol.* 8: 48–58.
4. Lachmann, P. J. 2009. The amplification loop of the complement pathways. *Adv. Immunol.* 104: 115–149.
5. Schmidt, C. Q., J. D. Lambris, and D. Ricklin. 2016. Protection of host cells by complement regulators. *Immunol. Rev.* 274: 152–171.
6. Zipfel, P. F., and C. Skerka. 1999. FHL-1/reconectin: a human complement and immune regulator with cell-adhesive function. *Immunol. Today* 20: 135–140.
7. Schmidt, C. Q., A. P. Herbert, D. Kavanagh, C. Gandy, C. J. Fenton, B. S. Blaum, M. Lyon, D. Uhrín, and P. N. Barlow. 2008. A new map of glycosaminoglycan and C3b binding sites on factor H. *J. Immunol.* 181: 2610–2619.
8. Schmidt, C. Q., A. P. Herbert, H. G. Hocking, D. Uhrín, and P. N. Barlow. 2008. Translational mini-review series on complement factor H: structural and functional correlations for factor H. *Clin. Exp. Immunol.* 151: 14–24.
9. Blackmore, T. K., T. A. Sadlon, H. M. Ward, D. M. Lublin, and D. L. Gordon. 1996. Identification of a heparin binding domain in the seventh short consensus repeat of complement factor H. *J. Immunol.* 157: 5422–5427.
10. Blackmore, T. K., J. Hellwage, T. A. Sadlon, N. Higgs, P. F. Zipfel, H. M. Ward, and D. L. Gordon. 1998. Identification of the second heparin-binding domain in human complement factor H. *J. Immunol.* 160: 3342–3348.
11. Herbert, A. P., J. A. Deakin, C. Q. Schmidt, B. S. Blaum, C. Egan, V. P. Ferreira, M. K. Pangburn, M. Lyon, D. Uhrín, and P. N. Barlow. 2007. Structure shows that a glycosaminoglycan and protein recognition site in factor H is perturbed by age-related macular degeneration-linked single nucleotide polymorphism. *J. Biol. Chem.* 282: 18960–18968.
12. Schmidt, C. Q., A. L. Hipgrave Ederveen, M. J. Harder, M. Wuhrer, T. Stehle, and B. S. Blaum. 2018. Biophysical analysis of sialic acid recognition by the complement regulator Factor H. *Glycobiology* 28: 765–773.
13. Prosser, B. E., S. Johnson, P. Roversi, A. P. Herbert, B. S. Blaum, J. Tyrrell, T. A. Jowitt, S. J. Clark, E. Tarelli, D. Uhrín, et al. 2007. Structural basis for complement factor H linked age-related macular degeneration. *J. Exp. Med.* 204: 2277–2283.
14. Morgan, H. P., C. Q. Schmidt, M. Guariento, B. S. Blaum, D. Gillespie, A. P. Herbert, D. Kavanagh, H. D. T. Mertens, D. I. Svergun, C. M. Johansson, et al. 2011. Structural basis for engagement by complement factor H of C3b on a self surface. *Nat. Struct. Mol. Biol.* 18: 463–470.
15. Kajander, T., M. J. Lehtinen, S. Hyvärinen, A. Bhattacharjee, E. Leung, D. E. Isenman, S. Meri, A. Goldman, and T. S. Jokiranta. 2011. Dual interaction of factor H with C3d and glycosaminoglycans in host-nonhost discrimination by complement. *Proc. Natl. Acad. Sci. USA* 108: 2897–2902.
16. Jokiranta, T. S., V.-P. Jaakola, M. J. Lehtinen, M. Pärepalo, S. Meri, and A. Goldman. 2006. Structure of complement factor H carboxyl-terminus reveals molecular basis of atypical haemolytic uremic syndrome. *EMBO J.* 25: 1784–1794.
17. Blaum, B. S., J. P. Hannan, A. P. Herbert, D. Kavanagh, D. Uhrín, and T. Stehle. 2015. Structural basis for sialic acid-mediated self-recognition by complement factor H. *Nat. Chem. Biol.* 11: 77–82.
18. Hyvärinen, S., S. Meri, and T. S. Jokiranta. 2016. Disturbed sialic acid recognition on endothelial cells and platelets in complement attack causes atypical hemolytic uremic syndrome. *Blood* 127: 2701–2710.
19. Schwaeble, W., J. Zwirner, T. F. Schulz, R. P. Linke, M. P. Dierich, and E. H. Weiss. 1987. Human complement factor H: expression of an additional truncated gene product of 43 kDa in human liver. *Eur. J. Immunol.* 17: 1485–1489.
20. Estaller, C., W. Schwaeble, M. Dierich, and E. H. Weiss. 1991. Human complement factor H: two factor H proteins are derived from alternatively spliced transcripts. *Eur. J. Immunol.* 21: 799–802.

21. de Córdoba, S. R., and E. G. de Jorge. 2008. Translational mini-review series on complement factor H: genetics and disease associations of human complement factor H. *Clin. Exp. Immunol.* 151: 1–13.
22. Józsi, M., S. Strobel, H.-M. Dahse, W. S. Liu, P. F. Hoyer, M. Oppermann, C. Skerka, and P. F. Zipfel. 2007. Anti factor H autoantibodies block C-terminal recognition function of factor H in hemolytic uremic syndrome. *Blood* 110: 1516–1518.
23. Józsi, M., M. Oppermann, J. D. Lambris, and P. F. Zipfel. 2007. The C-terminus of complement factor H is essential for host cell protection. *Mol. Immunol.* 44: 2697–2706.
24. Ferreira, V. P., A. P. Herbert, H. G. Hocking, P. N. Barlow, and M. K. Pangburn. 2006. Critical role of the C-terminal domains of factor H in regulating complement activation at cell surfaces. *J. Immunol.* 177: 6308–6316.
25. Ferreira, V. P., and M. K. Pangburn. 2007. Factor H mediated cell surface protection from complement is critical for the survival of PNH erythrocytes. *Blood* 110: 2190–2192.
26. Ferreira, V. P., A. P. Herbert, C. Cortés, K. A. McKee, B. S. Blaum, S. T. Esswein, D. Uhrín, P. N. Barlow, M. K. Pangburn, and D. Kavanagh. 2009. The binding of factor H to a complex of physiological polyanions and C3b on cells is impaired in atypical hemolytic uremic syndrome. *J. Immunol.* 182: 7009–7018.
27. Jokiranta, T. S., Z.-Z. Cheng, H. Seeberger, M. Jòzsi, S. Heinen, M. Noris, G. Remuzzi, R. Ormsby, D. L. Gordon, S. Meri, et al. 2005. Binding of complement factor H to endothelial cells is mediated by the carboxy-terminal glycosaminoglycan binding site. *Am. J. Pathol.* 167: 1173–1181.
28. Schmidt, C. Q., F. C. Slingsby, A. Richards, and P. N. Barlow. 2011. Production of biologically active complement factor H in therapeutically useful quantities. *Protein Expr. Purif.* 76: 254–263.
29. Ross, G. D., J. D. Lambris, J. A. Cain, and S. L. Newman. 1982. Generation of three different fragments of bound C3 with purified factor I or serum. I. Requirements for factor H vs CR1 cofactor activity. *J. Immunol.* 129: 2051–2060.
30. Schmidt, C. Q., H. Bai, Z. Lin, A. M. Risitano, P. N. Barlow, D. Ricklin, and J. D. Lambris. 2013. Rational engineering of a minimized immune inhibitor with unique triple-targeting properties. *J. Immunol.* 190: 5712–5721.
31. Harder, M. J., M. Anliker, B. Höchsmann, T. Simmet, M. Huber-Lang, H. Schrezenmeier, D. Ricklin, J. D. Lambris, P. N. Barlow, and C. Q. Schmidt. 2016. Comparative analysis of novel complement-targeted inhibitors, MiniFH, and the natural regulators factor H and factor H-like protein 1 reveal functional determinants of complement regulation. *J. Immunol.* 196: 866–876.
32. Jokiranta, T. S., J. Westin, U. R. Nilsson, B. Nilsson, J. Hellwage, S. Löfås, D. L. Gordon, K. N. Ekdahl, and S. Meri. 2001. Complement C3b interactions studied with surface plasmon resonance technique. *Int. Immunopharmacol.* 1: 495–506.
33. Wu, J., Y.-Q. Wu, D. Ricklin, B. J. C. Janssen, J. D. Lambris, and P. Gros. 2009. Structure of complement fragment C3b-factor H and implications for host protection by complement regulators. *Nat. Immunol.* 10: 728–733.
34. Sahu, A., S. N. Isaacs, A. M. Soulika, and J. D. Lambris. 1998. Interaction of vaccinia virus complement control protein with human complement proteins: factor I-mediated degradation of C3b to iC3b1 inactivates the alternative complement pathway. *J. Immunol.* 160: 5596–5604.
35. Yates, A., W. Akanni, M. R. Amode, D. Barrell, K. Billis, D. Carvalho-Silva, C. Cummins, P. Clapham, S. Fitzgerald, L. Gil, et al. 2016. Ensembl 2016. *Nucleic Acids Res.* 44(D1): D710–D716.
36. Nichols, E.-M., T. D. Barbour, I. Y. Pappworth, E. K. S. Wong, J. M. Palmer, N. S. Sheerin, M. C. Pickering, and K. J. Marchbank. 2015. An extended mini-complement factor H molecule ameliorates experimental C3 glomerulopathy. *Kidney Int.* 88: 1314–1322.
37. Xue, X., J. Wu, D. Ricklin, F. Forneris, P. Di Crescenzio, C. Q. Schmidt, J. Granneman, T. H. Sharp, J. D. Lambris, and P. Gros. 2017. Regulator-dependent mechanisms of C3b processing by factor I allow differentiation of immune responses. *Nat. Struct. Mol. Biol.* 24: 643–651.
38. Müller-Eberhard, H. J. 1986. The membrane attack complex of complement. *Annu. Rev. Immunol.* 4: 503–528.
39. Goicoechea de Jorge, E., J. J. E. Caesar, T. H. Malik, M. Patel, M. Colledge, S. Johnson, S. Hakobyan, B. P. Morgan, C. L. Harris, M. C. Pickering, and S. M. Lea. 2013. Dimerization of complement factor H-related proteins modulates complement activation in vivo. *Proc. Natl. Acad. Sci. USA* 110: 4685–4690.
40. Tortajada, A., H. Yébenes, C. Abarrategui-Garrido, J. Anter, J. M. García-Fernández, R. Martínez-Barricarte, M. Alba-Domínguez, T. H. Malik, R. Bedoya, R. Cabrera Pérez, et al. 2013. C3 glomerulopathy-associated CFHR1 mutation alters FHR oligomerization and complement regulation. *J. Clin. Invest.* 123: 2434–2446.
41. Caesar, J. J. E., H. Lavender, P. N. Ward, R. M. Exley, J. Eaton, E. Chittock, T. H. Malik, E. Goiecoechea De Jorge, M. C. Pickering, C. M. Tang, and S. M. Lea. 2014. Competition between antagonistic complement factors for a single protein on *N. meningitidis* rules disease susceptibility. *Elife* 3: e04008.
42. Józsi, M., A. Tortajada, B. Uzonyi, E. Goicoechea de Jorge, and S. Rodríguez de Córdoba. 2015. Factor H-related proteins determine complement-activating surfaces. *Trends Immunol.* 36: 374–384.
43. Tortajada, A., E. Gutiérrez, E. Goicoechea de Jorge, J. Anter, A. Segarra, M. Espinosa, M. Blasco, E. Roman, H. Marco, L. F. Quintana, et al. 2017. Elevated factor H-related protein 1 and factor H pathogenic variants decrease complement regulation in IgA nephropathy. *Kidney Int.* 92: 953–963.
44. van Beek, A. E., R. B. Pouw, M. C. Brouwer, G. van Mierlo, J. Geissler, P. Ooijevaar-de Heer, M. de Boer, K. van Leeuwen, T. Rispens, D. Wouters, and T. W. Kuijpers. 2017. Factor H-related (FHR)-1 and FHR-2 form *homo-* and heterodimers, while FHR-5 circulates only as homodimer in human plasma. *Front. Immunol.* 8: 1328.
45. Vik, D. P., J. B. Keeney, P. Muñoz-Cánoves, D. D. Chaplin, and B. F. Tack. 1988. Structure of the murine complement factor H gene. *J. Biol. Chem.* 263: 16720–16724.
46. Kühn, S., and P. F. Zipfel. 1996. Mapping of the domains required for decay acceleration activity of the human factor H-like protein 1 and factor H. *Eur. J. Immunol.* 26: 2383–2387.
47. Herzberger, P., C. Siegel, C. Skerka, V. Fingerle, U. Schulte-Spechtel, B. Wilske, V. Brade, P. F. Zipfel, R. Wallich, and P. Kraiczy. 2009. Identification and characterization of the factor H and FHL-1 binding complement regulator-acquiring surface protein 1 of the Lyme disease spirochete *Borrelia* spielmanii sp. nov. *Int. J. Med. Microbiol.* 299: 141–154.
48. Pangburn, M. K., and H. J. Müller-Eberhard. 1978. Complement C3 convertase: cell surface restriction of beta1H control and generation of restriction on neuraminidase-treated cells. *Proc. Natl. Acad. Sci. USA* 75: 2416–2420.
49. Kazatchkine, M. D., D. T. Fearon, and K. F. Austen. 1979. Human alternative complement pathway: membrane-associated sialic acid regulates the competition between B and beta1 H for cell-bound C3b. *J. Immunol.* 122: 75–81.
50. Meri, S., and M. K. Pangburn. 1990. Discrimination between activators and nonactivators of the alternative pathway of complement: regulation via a sialic acid/polyanion binding site on factor H. *Proc. Natl. Acad. Sci. USA* 87: 3982–3986.
51. Aslam, M., and S. J. Perkins. 2001. Folded-back solution structure of monomeric factor H of human complement by synchrotron X-ray and neutron scattering, analytical ultracentrifugation and constrained molecular modelling. *J. Mol. Biol.* 309: 1117–1138.
52. Oppermann, M., T. Manuelian, M. Józsi, E. Brandt, T. S. Jokiranta, S. Heinen, S. Meri, C. Skerka, O. Götze, and P. F. Zipfel. 2006. The C-terminus of complement regulator Factor H mediates target recognition: evidence for a compact conformation of the native protein. *Clin. Exp. Immunol.* 144: 342–352.
53. Schmidt, C. Q., A. P. Herbert, H. D. T. Mertens, M. Guariento, D. C. Soares, D. Uhrin, A. J. Rowe, D. I. Svergun, and P. N. Barlow. 2010. The central portion of factor H (modules 10-15) is compact and contains a structurally deviant CCP module. *J. Mol. Biol.* 395: 105–122.
54. Hebecker, M., M. Alba-Domínguez, L. T. Roumenina, S. Reuter, S. Hyvärinen, M.-A. Dragon-Durey, T. S. Jokiranta, P. Sánchez-Corral, and M. Józsi. 2013. An engineered construct combining complement regulatory and surface-recognition domains represents a minimal-size functional factor H. *J. Immunol.* 191: 912–921.
55. Herbert, A. P., E. Makou, Z. A. Chen, H. Kerr, A. Richards, J. Rappsilber, and P. N. Barlow. 2015. Complement evasion mediated by enhancement of captured factor H: implications for protection of self-surfaces from complement. *J. Immunol.* 195: 4986–4998.
56. Friese, M. A., J. Hellwage, T. S. Jokiranta, S. Meri, H. J. Müller-Quernheim, H. H. Peter, H. Eibel, and P. F. Zipfel. 2000. Different regulation of factor H and FHL-1/reconectin by inflammatory mediators and expression of the two proteins in rheumatoid arthritis (RA). *Clin. Exp. Immunol.* 121: 406–415.
57. Clark, S. J., C. Q. Schmidt, A. M. White, S. Hakobyan, B. P. Morgan, and P. N. Bishop. 2014. Identification of factor H-like protein 1 as the predominant complement regulator in Bruch's membrane: implications for age-related macular degeneration. *J. Immunol.* 193: 4962–4970.
58. Schwaeble, W., H. Schwaiger, R. A. Brooimans, A. Barbieri, J. Möst, M. Hirsch-Kauffmann, M. Tiefenthaler, D. F. Lappin, M. R. Daha, K. Whaley, et al. 1991. Human complement factor H. Tissue specificity in the expression of three different mRNA species. *Eur. J. Biochem.* 198: 399–404.
59. Gasque, P., M. Fontaine, and B. P. Morgan. 1995. Complement expression in human brain. Biosynthesis of terminal pathway components and regulators in human glial cells and cell lines. *J. Immunol.* 154: 4726–4733.
60. Junnikkala, S., T. S. Jokiranta, M. A. Friese, H. Jarva, P. F. Zipfel, and S. Meri. 2000. Exceptional resistance of human H2 glioblastoma cells to complement-mediated killing by expression and utilization of factor H and factor H-like protein 1. *J. Immunol.* 164: 6075–6081.
61. Junnikkala, S., J. Hakulinen, H. Jarva, T. Manuelian, L. Bjørge, R. Bützow, P. F. Zipfel, and S. Meri. 2002. Secretion of soluble complement inhibitors factor H and factor H-like protein (FHL-1) by ovarian tumour cells. *Br. J. Cancer* 87: 1119–1127.
62. Clark, S. J., S. McHarg, V. Tilakaratna, N. Brace, and P. N. Bishop. 2017. Bruch's membrane compartmentalizes complement regulation in the eye with implications for therapeutic design in age-related macular degeneration. *Front. Immunol.* 8: 1778.